

## BAYESIAN PROBABILITY THEORY IN ASTRONOMY: TIMING ANALYSIS OF THE GIANT FLARE OF SGR 1806–20

VALERI HAMBARYAN

*Astrophysical Institute and University Observatory  
Friedrich Schiller University of Jena, Germany  
E-mail: vvh@astro.uni-jena.de*

**Abstract.** For a photon-arrival times data sets the basics of a Bayesian statistical approach for detection and parameter estimation of periodic, variable and quasi-periodic oscillation (QPO) signal overviewed. An application to the complex data set of giant flare of Soft Gamma-ray Repeater (SGR) 1806–20 observed by *Rossi X-ray Timing Explorer (RXTE) Photon Counting Array (PCA)* on 27th of December 2004 is demonstrated. A comparison of Bayesian and classical approaches discussed.

### 1. INTRODUCTION

In X-ray and high energy astronomy modern instruments are able to register each individual photon. In particular, the position on the sky, energy of a photon, and its arrival time can be registered with very high accuracy.

This events can be very well described with a mathematical model *point processes*. First, they are point like in the sense of occupying a small and coextensive volume in the relevant space and secondly they are discrete, the degree to which they are distinct entities (Scargle and Babu 1998).

These photon arrival times, while not binned, are quantized in microsecond-scale units sometimes called "ticks" – since they are in fact generated by the ticking of the computer clock on-board of the spacecraft. In the approximation where the ticks are short compared to time scales of interest, they can be very accurately modeled by a Poisson process. Depending on the nature of the variability of the process, different mathematical models apply. For instance, a *constant* signal as *homogeneous* Poisson process, *deterministic (e.g. periodic)* as *inhomogeneous* and *random* as *doubly stochastic* ones.

Here, we present the results of a Bayesian approach of timing analysis of the giant flare data set of SGR 1806–20 registered on 2004 Dec 27 by *RXTE PCA*, having extremely complex shape of the light curve (see next section for description of the data set). The data are viewed as a point process in time, and analysis seeks to determine whether there are temporal variations modeled by abovementioned three types of poissonian processes.

## 2. SGR 1806–20 SUPER FLARE ON 27 Dec 2004

### 2.1. What are SGRs? State of the art

Over the last few years, a number of observational discoveries have again brought Magnetars (ultra-magnetized isolated neutron stars) to the forefront of researchers attention. These extreme objects comprise the Anomalous X-ray Pulsars (AXPs; 10 objects) and the Soft Gamma-ray Repeaters (SGRs; 5 objects), which are observationally very similar classes in many respects (for a recent review see Mereghetti 2008). They are all slow X-ray pulsars with spin periods clustered in a narrow range ( $P \sim 2\text{--}12\text{ s}$ ), relatively large period derivatives ( $\dot{P} \sim 10^{-13} - 10^{-10}\text{ s s}^{-1}$ ), spin-down ages of  $10^3 - 10^4\text{ yr}$ , and magnetic fields, as inferred from the classical magnetic dipole spin-down formula, of  $10^{14} - 10^{15}\text{ G}$ .

SGRs undergo periods of activity during which recurrent bursts with sub-second duration and peak luminosities of  $\sim 10^{38} - 10^{41}\text{ erg/s}$  are emitted. SGRs also show, on rare occasions, much more extreme events known as giant flares. These are characterized by an initial spike of duration comparable to that of recurrent bursts, but many orders of magnitude larger luminosity. Only three giant flares have so far been observed in over 30 yr of monitoring.

According to the magnetar model (Thompson and Duncan 1993, Thompson and Murray 2001) energy is fed impulsively to the neutron star magnetosphere when local "crustquakes" let magnetic helicity propagate outwards, giving rise to recurrent bursts with a large range of amplitudes. Giant flares are believed to originate from large-scale rearrangements of the inner field or catastrophic instabilities in the magnetosphere (Thompson and Duncan 2001, Lyutikov 2003). Most of this energy breaks out of the magnetosphere in a fireball of plasma expanding at relativistic speeds which results in the initial spike of giant flares. The decaying, oscillating tail that follows the spike displays many tens of cycles at the neutron star spin rate. This is interpreted as being due to a "trapped fireball" which remains anchored inside the magnetosphere and cools in a few minutes. The total energy released in this tail is  $\sim 10^{44}\text{ erg}$  in all three events detected so far.

Until 2004, the energy budget of SGRs and AXPs was believed to be dominated by their persistent emission at a level of  $\sim 10^{35}\text{ erg s}^{-1}$ . This translated into an internal field of  $\sim 10^{15}\text{ G}$ . The properties of the 2004 Dec 27 giant flare from SGR1806-20 imply that the emission budget of Magnetars is dominated by giant flares, see e.g. Stella et al. (2009). This therefore has important implications for several subjects at the forefront of research.

A power spectrum analysis of the high time resolution data from the 2004 Dec 27 event of SGR1806-20, observed with the X-Ray Timing Explorer (RXTE), led to the discovery of fast Quasi Periodic Oscillations (QPOs) in the X-ray flux of the decaying tail of SGR (Israel et al. 2005). QPOs of different frequencies were detected, some of which were active simultaneously and displayed highly significant QPO signals at about 18, 26, 30, 93, 150, 625 and 1840 Hz (Watts and Strohmayer 2006). A re-analysis of the decaying tail data from the 1998 giant flare of another Magnetar, SGR 1900+14, revealed QPOs around frequencies of 28, 54, 84 and 155 Hz (Strohmayer and Watts 2006). Hints for a signal at  $\sim 43\text{ Hz}$  in the March 1979 event from SGR

0526-66 were reported as early as 1983 (Barat et al. 1983). All QPO signals show large amplitude variations with time and especially with the phase of the stars rotational modulation.

## 2.2. Observational data

The giant flare of SGR 1806–20 has been observed by many space based missions. The data recorded by *RXTE PCA* instrument, consisting of five Xenon-filled detectors covering the energy range 2–50 keV, used the configuration GoodXenon, which records all good events detected in the Xenon chamber with full timing accuracy of 1  $\mu$ s. Publicly available data were retrieved by the *XTE Data Finder* (XDF) user interface (Rots and Hilldrup 1997). Event data files have been created and photon arrival times were corrected for the solar barycenter using scripts provided in the package *XTE ftools*. The data set consists of 698770 registered photons. However, during the initial intensive spike phase of the giant flare the detectors were saturated. For that reason, in our analysis we use the data after  $\sim 8.9$ sec of the flare onset, consisting of  $\sim 650000$  photon arrival times, clearly covering 51 rotational cycles of SGR 1806–20 (see Fig. 1).

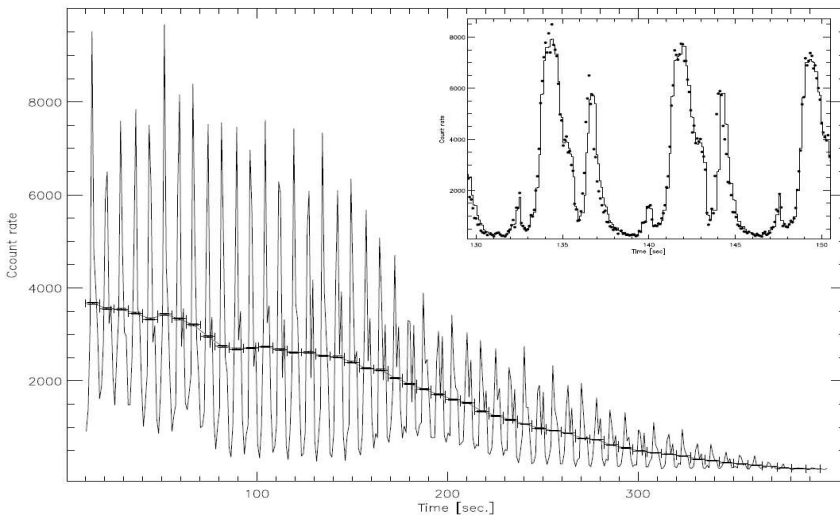


**Figure 1.** Light curve of the *RXTE* giant flare of SGR 1806–20 observed on 27th of December 2004. The general decay of the giant flare with a bumpy structure on top of it, namely a strongly periodic signal due to rotation (7.56 sec). The inset panel shows the rotational modulated light curve (filled circles) together with fitted piecewise constant model (solid line) (Hutter 2007), shown here only for 2.5 rotational cycles, with a very complex light curve structure. See text for details.

It is clear that observational detection and parameter estimation of QPO frequencies may play a crucial role for testing any theory predicting eigenfrequencies of the neutron star. In this connection, timing analysis of complex flare data set of SGR 1806–20, with the aim of QPO detection, may be divided into several mutually con-

nected, challenging problems. They include the significance of quasi-periodic signal detection and parameter estimation with high precision. Indeed, the decaying tail, of the giant flare of SGR 1806–20, itself has a bumpy structure, very complex light curve shape modulated by rotation of the neutron star (see Fig. 1).

Thus, for investigation of this dataset a procedure properly should take into account all these variations.

### 2.3. Timing analysis with a Bayesian change point detection method

In order to study the changes of the photon arrival times (variability detection) we performed a timing analysis of the datasets using a Bayesian change point detection method<sup>1</sup> developed by Scargle (1998, 2000). This method is well suited for a statistical examination when the arrival times of individual X-ray photons are registered (see Hambaryan et al. 1999, Schwöpe et al. 2002). It is superior to methods which work on binned data, since it requires no a priori knowledge of the relevant time-scale of the variability structure which will be investigated.

Scargle’s (1998, 2000) method decomposes a given set of photon counting data into Bayesian blocks with piecewise constant count-rate according to Poisson statistics. Bayesian blocks are built by a Cell Coalescence algorithm (Scargle 2000), which begins with a fine-grained segmentation. It uses a Voronoi tessellation<sup>2</sup> of data points, where neighboring cells are merged if allowed by the corresponding marginal likelihoods (Scargle 2000).

We repeat here the essential parts of the method, expanding upon particular modifications of the original method as used in the present application. Assume that during a continuous observational interval of length  $T$ , consisting of  $m$  discrete moments in time (spacecraft’s ”clock tick”), a set of photon arrival times  $D (t_i, t_{i+1}, \dots, t_{i+n})$  is registered. Suppose now that we want to use these data to compare two competing hypotheses, The first hypothesis is that the data are generated from a constant rate Poisson process (model  $M_1$ ) and the second one from two-rate Poisson process (model  $M_2$ ). Evidently, model  $M_1$  is described by only one parameter  $\theta$  (the count rate) of the one rate Poisson process while the model  $M_2$  is described by parameters  $\theta_1$ ,  $\theta_2$  and  $\tau$ . The parameter  $\tau$  is the time when the Poisson process switches from  $\theta_1$  to  $\theta_2$  during the total time  $T$  of observation, which thus is divided in intervals  $T_1$  and  $T_2$ .

By taking as a background information ( $I$ ) the proposition that one of the models under consideration is true and by using Bayes’ theorem we can calculate the posterior probability of each model by (the probability that  $M_k$  ( $k = 1, 2$ ) is the correct model, see, e.g., Jaynes and Bretthorst 2003)

$$Pr(M_k|D, I) = \frac{Pr(D|M_k, I)}{Pr(D|I)} Pr(M_k|I) \quad (1)$$

where  $Pr(D|M_k, I)$  is the (marginal) probability of the data assuming model  $M_k$ , and  $Pr(M_k|I)$  is the prior probability of model  $M_k$  ( $k = 1, 2$ ). The term in the

<sup>1</sup>In general terms, the change-point methodology deals with sets of sequentially ordered observations (as in time) and determines whether the fundamental mechanism generating the observations has changed during the time the data have been gathered (see, e.g. Csörgő and Horváth 1997).

<sup>2</sup>The Voronoi cell for a data point consists of all the space closer to that point than to any other data point.

denominator is a normalization constant, and we may eliminate it by calculating the ratio of the posterior probabilities instead of the probabilities directly. Indeed, the extent to which the data support model  $M_2$  over  $M_1$  is measured by the ratio of their posterior probabilities and is called the posterior odds ratio

$$O_{21} \equiv \frac{Pr(M_2|D, I)}{Pr(M_1|D, I)} = \left[ \frac{Pr(D|M_2, I)}{Pr(D|M_1, I)} \right] \left[ \frac{Pr(M_2|I)}{Pr(M_1|I)} \right]. \quad (2)$$

The first factor on the right-hand side of Eq. (2) is the ratio of the *integrated* or *global* likelihoods of the two models and is called the *Bayes factor* for  $M_2$  against  $M_1$ , denoted by  $B_{21}$ . The global likelihood for each model can be evaluated by integrating over nuisance parameters and the final result for discrete Poisson events can be represented by (see, for details, Scargle 1998, 2000, Hambaryan et al. 1999).

$$B_{21} = \frac{1}{B(n+1, m-n+1)} \sum B(n_1+1, m_1-n_1+1) \times B(n_2+1, m_2-n_2+1) \Delta\tau, \quad (3)$$

where  $B$  is the *beta function*,  $n_j$  and  $m_j$ , ( $j = 1, 2$ ), respectively are the number of recorded photons and the number of "clock ticks" in the observation intervals of lengths  $T_1$  and  $T_2$ .  $\Delta\tau$  is the time interval between successive photons, and the sum is over the photons' index.

The second factor on the right-hand side of Eq. (2) is the prior odds ratio, which will often be equal to 1 (see below), representing the absence of an *a priori* preference for either model.

It follows that the Bayes factor is equal to the posterior odds when the prior odds is equal to 1. When  $B_{21} > 1$ , the data favor  $M_2$  over  $M_1$ , and when  $B_{21} < 1$  the data favor  $M_1$ .

If we have calculated the odds ratio  $O_{21}$ , in favor of model  $M_2$  over  $M_1$ , we can find the probability for model  $M_2$  by inverting Eq. (2), giving

$$Pr(M_2|D, I) = \frac{O_{21}}{1 + O_{21}}. \quad (4)$$

Applying this approach to the observational data set, Scargle's (1998, 2000) method returns an array of rates,  $(\theta_1, \theta_2, \dots, \theta_{cp})$ , and a set of so called "change points"  $(\tau_1, \tau_2, \dots, \tau_{cp-1})$ , giving the times when an abrupt change in the rate is determined, i.e. a significant variation. This is the most probable partitioning of the observational interval into blocks during which the photon arrival rate displayed no statistically significant variations.

In Fig. 1 we visualize the outcome of the application to the observational data set, that divided it into time intervals (segments/blocks) within each of them a signal can be considered as a constant with poissonian noise. In contrary, between those intervals significant change of the observed count rate occurred.

Thus, next we may perform a search for a periodic/quasi-periodic signal taking into account this segmentation.

## 2.4. The Gregory-Loredo (Bayesian) method for periodicity search.

The most widely-used procedure for detection of QPOs is an analysis of the power spectrum calculated from the fast Fourier transform (FFT) of uniformly sampled data. Application of the FFT to arrival time series data requires binning of the data to produce equally spaced samples. Binning is a subjective procedure; the choice of the bin width and edges can affect the apparent significance of a detection and limits sensitivity on short time scales. Moreover, the presence of the so-called red-noise (low frequency signal in the data, i.e. high calculated power can appear at low frequency because of long-timescale features of the data and at high frequencies from higher harmonics of complex shape strong periodic signal) may cause certain problems with the interpretation of the results (e.g. Bretthorst 1988). In the previous timing analysis of the giant flare data set of SGR 1806–20 by Israel et al. (2005) and Watts and Strohmayer (2006), an averaged power spectrum was considered. Namely, for each rotational cycle or certain rotational phase interval of SGR 1806–20 an independent classical power spectrum was determined depending on the phase of rotation and decaying tail of the giant flare, which were co-added and averaged subsequently. This approach divides the data set into small time intervals, which automatically reduces the significance of any periodicity detection and nearly takes into account the complex shape of the data set (rotational modulation and decaying tail of flare light curves, Fig. 1). Moreover, in some circumstances it may fail to detect the periodic signal (see e.g. Gregory and Loredo 1996). Indeed, as explicitly shown by Jaynes (1987) (see also, Bretthorst 1988, 2001, Gregory 2005) the probability for the frequency of a periodic sinusoidal signal is given approximately by

$$p(f_n|D, I) \propto \exp\left[\frac{C(f_n)}{\sigma^2}\right], \quad (5)$$

where  $C(f_n)$  is the squared magnitude of the FFT.

To avoid subjectivity and loss of sensitivity, we used a procedure which does not require binning and takes into consideration the rotational modulation and decaying tail of the flare (Bretthorst 1988, Gregory and Loredo 1992, 1996, Jaynes and Bretthorst 2003, Vaughan 2009).

For the analysis of the data for the search of QPOs during the giant flare of SGR 1806–20, we applied a Bayesian method developed by Gregory and Loredo (1992) (hereafter referred to as the GL method) for the search of pulsed emission from pulsars in X-ray data, consisting of the arrival times of events, when we have no specific prior information about the shape of the signal.

The GL method for timing analysis first tests if a constant, variable or periodic signal is present in a data set. As a particular case of a QPO<sup>3</sup> can be considered a periodic signal with some length of coherence, i.e. a periodic signal with additional parameters of the oscillation with start and end times. In the GL method, periodic models are represented by a signal folded into trial frequency with a light curve shape as a stepwise function with  $m$  phase bins per period plus a noise contribution. With

---

<sup>3</sup>A QPO can be the result of a random process with a continuous power spectrum that contains a broad peak, or a locally monochromatic periodic signal, the frequency of which changes over time, either randomly or deterministically, or a combination of these.

such a model we are able to approximate a light curve of any shape. Hypotheses for detecting periodic signals represents a class of stepwise periodic models with the following parameters: trial period, phase, noise parameter and number of bins ( $m$ ). The most probable model parameters are then estimated by marginalization of the posterior probability over the prior specified range of each parameter. In Bayesian statistics posterior probability contains a term that penalizes complex models (unless there is no significant evidence to support that hypothesis), hence we calculate the posterior probability by marginalizing over a range of models, corresponding to a prior range of number of phase bins,  $m$ , from 2 to 12. Moreover, the GL method is well suited for variability detection, i.e. to characterize an arbitrary shape light curve with piecewise constant function  $Z(t)$  (Rots 2006).

For the search and detection of QPOs we used a slightly different version of the GL method (Hambaryan et al. 2010). First we determined  $Z(t)$  - apodizing or weighting function (fitting with a piecewise constant model to characterize the complex light curve shape in the data set, giant flare decaying tail and rotational modulated light curve, see also previous section). Then we subsequently compare competing hypothesis, i.e. whether the data support a purely piecewise constant or piecewise constant+periodic model. If there is an indication of the presence of a periodic signal we determine also the time intervals where it has its maximum strength (e.g. amplitude or pulsed fraction) via a Markov Chain Monte Carlo (MCMC) approach using QPO start and end times as free parameters.

Finally, in the latter case, we estimate parameters (frequency, phase, amplitude, coherence length of QPO, etc.) of the periodic signal with high precision, using the posterior probabilities of frequencies in a periodic signal:

$$p(\omega|D, M_m) = \frac{C}{\omega} \int_0^{2\pi} d\phi \frac{1}{W_m(\omega, \phi)}, \quad (6)$$

where  $C = \left[ \int_{\omega_{lo}}^{\omega_{hi}} \frac{d\omega}{\omega} \int_0^{2\pi} d\phi \frac{1}{W_m(\omega, \phi)} \right]^{-1}$  and  $W_m(\omega, \phi) = \frac{N!}{n_1!n_2!\dots n_m!}$  are the normalization constant and number of ways the binned distribution could have arisen "by chance".  $n_j(\omega, \phi)$  is the number of events falling into the  $j$ th of  $m$  phase bins given the frequency,  $\omega$ , and phase,  $\phi$ .  $N$  is the total number of photons (for details, see Gregory and Loredo 1992).

First, we applied the GL method as implemented by Gregory and Loredo (1992) to the 2004 Dec 27 giant flare whole data set of SGR 1806–20 observed by *RXTE PCA* and started the timing analysis by performing a blind periodicity search in the range of 12.0-160 Hz. Naturally, we found a very strong coherent signal at  $\sim 7.56$ s, the pulsation period of the NS, followed by higher harmonics up to the 100Hz (see Fig. 2), which have to be excluded as potential QPO frequencies triggered by other phenomenon different than rotation of NS.

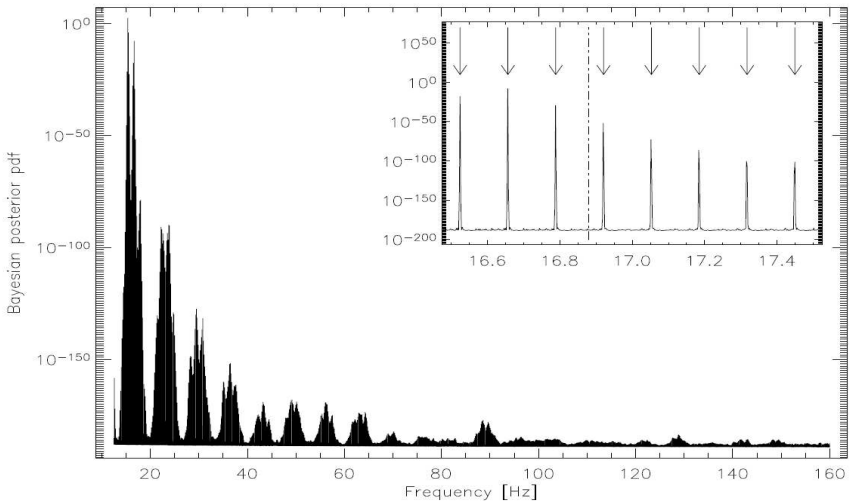


**Figure 2.** Application of the GL method for blind periodicity search to the complete data set obtained by *RXTE PCA* of giant flare of SGR 1806–20 2004 Dec 27 revealed a strong coherent signal at the frequency of 0.13219244 Hz and higher harmonics up to 100Hz. Bayesian posterior probability density vs frequencies in the range of 12.0–160 Hz is shown. The inset panel shows a zoomed part of it around 16.88 Hz. Arrows are indicating higher harmonics (from 125 to 132) of the fundamental frequency and the dash-dotted vertical line shows one of the detected QPO frequency in a short time interval (see text, for details).

Next, we divided the data set into 51 rotational cycles (see Fig. 1). Each of these subsamples were treated as independent data sets. We determined the Bayesian probability densities versus trial frequency. Final probabilities were derived in two ways. First, as the likelihood of those independent Bayesian posterior probability density functions and the second one simply summing those independent probabilities<sup>4</sup> (see Fig. 3).

This approach also revealed a number of rotational cycles within which the probability of the model of periodic signal is significantly higher than the constant one. Namely, during time intervals of 183.8–191.2, 244.3–251.9 and 259.4–267.1 seconds, from the flare onset, odds ratios of periodic vs constant models are  $\sim 10$ ,  $\sim 30$  and  $\sim 197$ , correspondingly.

<sup>4</sup>Addition rule of probabilities: probability that the QPOs at the given frequency are present  $\Delta t_1$  or  $\Delta t_2$  or both time intervals, while likelihood (i.e. summed power spectrum) defines the probability of presence QPOs during  $\Delta t_1$  and  $\Delta t_2$  (i.e. multiplication rule of probabilities, see also, Eq. 5)



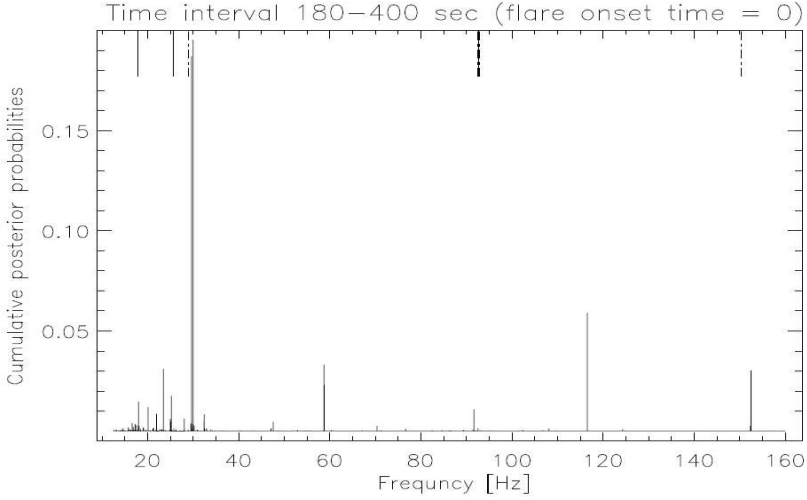


**Figure 3.** The Bayesian posterior probability density vs. trial frequency of the periodic signal for the giant flare data set of SGR 1806–20. QPO frequencies already detected by averaged power spectrum analysis and also with other mission *RHESSI* (Israel et al. 2005, Watts and Strohmayer 2006) are marked as small lines at the top axis. Those QPO frequencies are also detected by us. In addition, we have detected several more QPO frequencies (21, 59 and 116 Hz) with the Bayesian method, which were also predicted by Colaiuda et al. (2009).

In order to detect QPO start and end times we included also observational data of neighbouring rotational cycles (where a QPO with that frequency was not detected) and performed the periodicity search for an expanded time interval with additional two free parameters with the MCMC approach with Metropolis-Hastings algorithm. As initial values of these ( $t_{QPOstart}$  and  $t_{QPOend}$ ) parameters served start and end times of an observation, satisfying the condition:  $t_{Obs.start} \leq t_{QPOstart} < t_{QPOend} \leq t_{Obs.end}$ . In principle, starting with the abovementioned initial values can be considered as a good strategy, since the detected signal has a higher significance in a subinterval of the considered time interval and the fast convergence of the MCMC procedure already provided. This analysis via MCMC revealed even shorter time intervals within which periodic signal is stronger. The estimates of QPO frequencies and the corresponding 68% interval of the highest probability densities are presented in the Table 1 (see, also Fig. 4, 5).

**Table 1:** Detected QPO frequencies not reported in the literature (Israel et al. 2005, Watts and Strohmayer 2006, Strohmayer and Watts 2006).

| $f_{QPO}$ [Hz] ( 68% credible region) | Time intervals of detected QPOs <sup>a</sup> |
|---------------------------------------|--|
| 16.88 <sup>b</sup> (16.87 – 16.90)    | 259.4-267.1                                  |
| 21.36 <sup>b</sup> (21.35 – 21.38)    | 244.3-251.9                                  |
| 36.84 <sup>b</sup> (36.83 – 36.88)    | 183.8-191.2                                  |
| 59.04 (58.58 – 59.28)                 | 146.0-176.2                                  |
| 61.26 (61.25 – 61.27)                 | 251.9-395.6                                  |
| 116.27 (116.24 – 116.28)              | 168.7-198.9                                  |

<sup>a</sup> Giant Flare onset time is set to 0

<sup>b</sup> Highly significant detection (for details, see text)

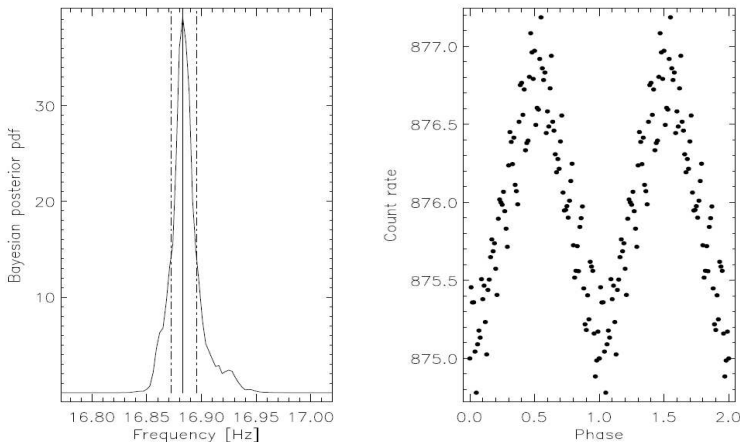


**Figure 4.** Bayesian posterior probability density vs frequencies in the time interval of 259-267 sec from the giant flare onset. By dashed vertical lines are indicated the 68% region of the highest probability density. Odds-ratio of periodic vs constant model is  $\sim 200$ . The right panel depicts the phase folded light curve with frequency  $f_{QPO} = 16.88\text{Hz}$ , it has almost perfect sinusoidal shape (for details, see text).

### 3. RESULTS

We report the detection of QPOs from SGR 1806–20 giant flare decaying tail recorded by the *RXTE* PCA by applying the GL method for periodicity search. We have confirmed the detections of QPOs at frequencies (in the range of 12 – 160Hz) reported by Watts and Strohmayer (2006) and, in addition, we found some more QPOs at  $f_{QPOs} = 16.9, 21.4, 36.8\text{Hz}$  with corresponding odds ratios  $\sim 197, \sim 30$  and  $\sim 10$ , in shorter time scales, i.e. within individual rotational cycles (see, Fig. 5). These odds ratios, describing the significance of presence of a periodic signal, are sensitive

to the frequency search range. In contrast, detected frequencies of QPOs, found by locating maximums in the posterior probability density function, are insensitive to the prior search range of frequencies. We computed the uncertainty of  $f_{QPOs}$  at 68% confidence level ("posterior bubble") by using this posterior probability density function. In addition to that, we have also estimated the significance of our QPO detection by an empirically determined cumulative distribution (see, Fig. 5).

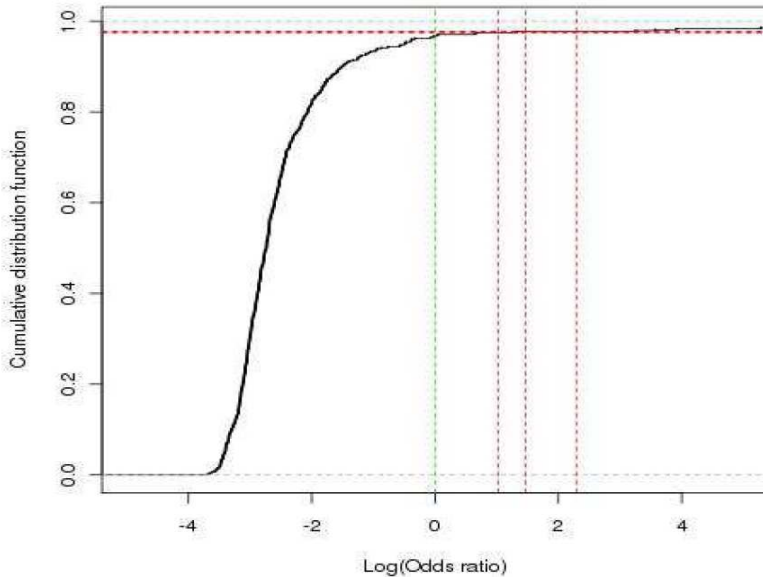


**Figure 5.** Empirical cumulative distribution function as a function of Odds ratio, i.e. the probability of periodic model vs constant one, on the base of simulations of QPO frequencies with different amplitudes and noise, as much as possible to the observed values in terms of number of registered photons, spanned times, etc.. Detected QPO frequencies indicated by vertical dashed lines, showing a high significance of detections.

The broad variety of neutron star oscillation modes (McDermott et al. 1985) is associated with their global structure as well as their internal characteristics. Neutron star seismology has already been proposed as a tool to understand their internal structure (Kokkotas et al. 2001). The various types of oscillations carry information about the equation of state, the thickness of the crust, the mass, radius and even the rotation rate (Gaertig and Kokkotas 2010). Still, modeling a truly realistic oscillating neutron star is difficult, however the potential reward is considerable. This has been demonstrated from the recent theoretical results for the QPOs which have been interpreted as magnetoelastic oscillations. These calculations have shown how the observations constrain both the mass, the radius, the thickness of the crust and the strength of magnetic field of these stars (Sotani et al. 2007, Samuelsson and Andersson 2007, Colaiuda et al. 2009, Cerdá-Durán et al. 2009). While one could even set severe constraints in the geometry of the interior magnetic field (see Sotani et al. 2008).

In particular, by studying Alfvén oscillations (Colaiuda et al. 2009) could find in the magnetar interior that there were no discrete modes but instead a continuum (as suggested by Levin 2007). The edges of this continuum have been used to explain the observed QPOs. It is worth noticing, that QPO frequencies found in this work have been predicted by Colaiuda et al. (2009).

Thus, by application of Bayesian approach to the photon arrival dataset of the giant flare of SGR 1806–20 (variability and periodicity search):

1. We found new QPOs applying a Bayesian timing analysis method of the decaying tail of the giant flare of SGR 1806–20 2004 Dec 27, observed by *RXTE PCA*, not yet reported in the literature.
2. Some of these QPO frequencies ( $f_{QPOs} \sim 17, 22, 37, 56, 112\text{Hz}$ ) are predicted by the theoretical study of torsional Alfvén oscillations of magnetars (see, Table 2, by Colaiuda et al. 2009), suggesting  $APR_{14}$  (Akmal et al. 1998) EoS<sup>5</sup> of SGR 1806–20.
3. These preliminary results are very promising and we plan to extend our high frequency oscillations research (both the theoretical predictions as well as the observations) to both activity periods, as well as to the quiescent state of SGRs and AXPs, as well as to the isolated neutron stars with comparatively smaller magnetic fields.

### Acknowledgements

We acknowledge support by the German *Deutsche Forschungsgemeinschaft (DFG)* through project C7 of SFB/TR 7 "Gravitationswellenastronomie" This research has made use of data obtained from the High Energy Astrophysics Science Archive Research Center (HEASARC) provided by NASA's Goddard Space Flight Center.

### References

- Akmal, A., Pandharipande, V. R. and Ravenhall, D. G.: 1998, Equation of state of nucleon matter and neutron star structure, *Physical Review C*, **58**, 1804, arXiv:hep-ph/9804388.
- Barat, C., Hayles, R. I., Hurley, K., Niel, M., Vedrenne, G., Desai, U., Kurt, V. G., Zenchenko, V. M. and Estulin, I. V.: 1983, Fine time structure in the 1979 March 5 gamma ray burst, *A&A*, **126**, 400.
- Bretthorst, G. L.: 1988, Bayesian Spectrum Analysis and Parameter Estimation, Springer-Verlag, New York.
- Bretthorst, G. L.: 2001, Generalizing the Lomb-Scargle periodogram. In Bayesian Inference and Maximum Entropy Methods in Science and Engineering, edited by A. Mohammad-Djafari (2001), *American Institute of Physics Conference Series*, **568**, pp. 241-245.
- Cerá-Durán, P., Stergioulas, N. and Font, J. A.: 2009, Alfvén QPOs in magnetars in the anelastic approximation, *MNRAS*, **397**, 1607, 0902.1472.
- Colaiuda, A., Beyer, H. and Kokkotas, K. D.: 2009, On the quasi-periodic oscillations in magnetars, *MNRAS*, **396**, 1441, 0902.1401.
- Csörgő, M. and Horváth, L. editors: 1997, Limit theorems in change point analysis, Wiley.

---

<sup>5</sup>Neutron star models based on the models for the nucleon-nucleon interaction with the inclusion of a parameterized three-body force and relativistic boost corrections, estimating maximum mass and stiffness (see, also Heiselberg and Hjorth-Jensen 1999).

- Gaertig, E. and Kokkotas, K. D.: 2010, Gravitational wave asteroseismology with fast rotating neutron stars, ArXiv e-prints 1005.5228.
- Gregory, P. C.: 2005, Bayesian Logical Data Analysis for the Physical Sciences: A Comparative Approach with 'Mathematica' Support, Cambridge University Press.
- Gregory, P. C. and Loredo, T. J.: 1992, A new method for the detection of a periodic signal of unknown shape and period, *ApJ*, **398**, 146.
- Gregory, P. C. and Loredo, T. J.: 1996, Bayesian Periodic Signal Detection: Analysis of ROSAT Observations of PSR 0540-693, *ApJ*, **473**, 1059.
- Hambaryan, V., Neuhäuser, R. and Kokkotas, K. D.: 2010, Bayesian timing analysis of giant flare of SGR 1806-20 by RXTE PCA. ArXiv e-prints 1012.5654.
- Hambaryan, V., Neuhäuser, R. and Stelzer, B.: 1999, Bayesian flare event detection. ROSAT X-ray observations of the UV Cetus type star G 131-026, *A&A*, **345**, 121.
- Heiselberg, H. and Hjorth-Jensen, M.: 1999, Phase Transitions in Neutron Stars and Maximum Masses, *ApJL*, **525**, L45, arXiv:astro-ph/9904214.
- Hutter, M.: 2007, Exact Bayesian Regression of Piecewise Constant Functions, Bayesian Analysis 2(4), 635, URL <http://arxiv.org/abs/math.ST/0606315>.
- Israel, G. L., Belloni, T., Stella, L., Rephaeli, Y., Gruber, D. E., Casella, P., Dall'Osso, S., Rea, N., Persic, M. and Rothschild, R. E.: 2005, The Discovery of Rapid X-Ray Oscillations in the Tail of the SGR 1806-20 Hyperflare, *ApJL*, **628**, L53, arXiv:astro-ph/0505255.
- Jaynes, E. T.: 1987, Bayesian spectrum and chirp signals. In In Proc. Maximum Entropy and Bayesian Spectral Analysis, pp. 1-37.
- Jaynes, E. T. and Bretthorst, G. L.: 2003, Probability Theory, Cambridge University Press.
- Kokkotas, K. D., Apostolatos, T. A. and Andersson, N.: 2001, The inverse problem for pulsating neutron stars: a 'fingerprint analysis' for the supranuclear equation of state, *MNRAS*, **320**, 307, arXiv:gr-qc/9901072.
- Levin, Y.: 2007, On the theory of magnetar QPOs, *MNRAS*, **377**, 159, arXiv:astro-ph/0612725.
- Lyutikov, M.: 2003, Explosive reconnection in magnetars, *MNRAS*, **346**, 540, arXiv:astro-ph/0303384.
- McDermott, P. N., van Horn, H. M., Hansen, C. J. and Buland, R.: 1985, The nonradial oscillation spectra of neutron stars, *ApJL*, **297**, L37.
- Mereghetti, S.: 2008, The strongest cosmic magnets: soft gamma-ray repeaters and anomalous X-ray pulsars, *A&AR*, **15**, 225, 0804.0250.
- Rots, A. H.: 2006, Effectiveness of the Gregory-Loredo Algorithm for the Detection of Temporal Variability in Chandra Data. In Astronomical Data Analysis Software and Systems XV, edited by C. Gabriel, C. Arviset, D. Ponz, & S. Enrique, *Astronomical Society of the Pacific Conference Series*, **351**, pp. 73–+.
- Rots, A. H. and Hildrup, K. C.: 1997, The XTE Data Finder (XDF). In Astronomical Data Analysis Software and Systems VI, edited by G. Hunt & H. Payne, volume 125 of *Astronomical Society of the Pacific Conference Series*, pp. 275–+.
- Samuelsson, L. and Andersson, N.: 2007, Neutron star asteroseismology. Axial crust oscillations in the Cowling approximation, *MNRAS*, **374**, 256, arXiv:astro-ph/0609265.
- Scargle, J. D.: 1998, Studies in Astronomical Time Series Analysis. V. Bayesian Blocks, a New Method to Analyze Structure in Photon Counting Data, *ApJ*, **504**, 405.
- Scargle, J. D.: 2000, Bayesian Blocks: Divide and Conquer, MCMC, and Cell Coalescence Approaches, ArXiv Physics e-prints. arXiv:physics/0009033.
- Scargle, J. D. and Babu, G. J.: 1998, Point Processes in Astronomy: Exciting Events in the Universe. preprint.
- Schwope, A. D., Hambaryan, V., Schwarz, R., Kanbach, G. and Gänsicke, B. T.: 2002, A multiwavelength timing analysis of the eclipsing polar DP Leo, *A&A*, **392**, 541, arXiv:astro-ph/0111457.
- Sotani, H., Colaiuda, A. and Kokkotas, K. D.: 2008, Constraints on the magnetic field geometry of magnetars, *MNRAS*, **385**, 2161, 0711.1518.
- Sotani, H., Kokkotas, K. D. and Stergioulas, N.: 2007, Torsional oscillations of relativistic stars with dipole magnetic fields, *MNRAS*, **375**, 261, arXiv:astro-ph/0608626.

- Stella, L., Dall’Osso, S. and Israel, G. L.: 2009, The giant flare of 2004 Dec 27 from SGR1806-20 and fundamental physics from magnetars, *Memorie della Societa Astronomica Italiana*, **80**, 186.
- Strohmayer, T. E. and Watts, A. L.: 2006, The 2004 Hyperflare from SGR 1806-20: Further Evidence for Global Torsional Vibrations, *ApJ*, **653**, 593, arXiv:astro-ph/0608463.
- Thompson, C. and Duncan, R. C.: 1993, Neutron star dynamos and the origins of pulsar magnetism, *ApJ*, **408**, 194.
- Thompson, C. and Duncan, R. C.: 2001, The Giant Flare of 1998 August 27 from SGR 1900+14. II. Radiative Mechanism and Physical Constraints on the Source, *ApJ*, **561**, 980, arXiv:astro-ph/0110675.
- Thompson, C. and Murray, N.: 2001, Transport of Magnetic Fields in Convective, Accreting Supernova Cores, *ApJ*, **560**, 339, arXiv:astro-ph/0105425.
- Vaughan, S.: 2009, A Bayesian test for periodic signals in red noise, *MNRAS*, pp. 1752–+, 0910.2706.
- Watts, A. L. and Strohmayer, T. E.: 2006, Detection with RHESSI of High-Frequency X-Ray Oscillations in the Tail of the 2004 Hyperflare from SGR 1806-20, *ApJl*, **637**, L117, arXiv:astro-ph/0512630.